J. Microbiol. Biotechnol. (1999), **9**(5), 593–603

JOURNAL OF
MICROBIOLOGY
AND
BIOTECHNOLOGY

Metabolic Analysis of Poly(3-Hydroxybutyrate) Production by Recombinant *Escherichia coli*

WONG, HENG HO[†], RICHARD J. VAN WEGEN[2,†], JONG-IL CHOI, SANG YUP LEE[*], AND ANTON P. J. MIDDELBERG[1]

Department of Chemical Engineering and Bioprocess Engineering Research Center, Korea Advanced Institute of Science and Technology, 373-1 Kusong-Dong, Yusong-Gu, Taejon 305-701, Korea
[1]Department of Chemical Engineering, University of Cambridge, Pembroke Street, Cambridge, CB2 3RA, U.K.
[2]Department of Chemical Engineering, University of Adelaide, SA 5005, Australia

Received: June 3, 1999

Abstract Poly(3-hydroxybutyrate) (PHB) production by fermentation was examined under both restricted- and ample-oxygen supply conditions in a single fed-batch fermentation. Recombinant *Escherichia coli* transformed with the PHB production plasmid pSYL107 was grown to reach high cell density (227 g/l dry cell weight) with a high PHB content (78% of dry cell weight), using a glucose-based minimal medium. A simple flux model containing 12 fluxes was developed and applied to the fermentation data. A superior closure (95%) of the carbon mass balance was achieved. When the data were put into use, the results demonstrated a surprisingly large excretion of formate and lactate. Even though periods of severe oxygen limitation coincided with rapid acetate and lactate excretion, PHB productivity and carbon utilization efficiency were not significantly impaired. These results are very positive in reducing oxygen demand in an industrial PHA fermentation without sacrificing its PHA productivity, thereby reducing overall production costs.

Key words: *Escherichia coli*, metabolic flux analysis, poly-(3-hydroxybutyrate), oxygen limitation, fermentation, high cell density culture

Polyhydroxyalkanoates (PHAs), the most common of which is poly(3-hydroxybutyrate) (PHB), show an excellent choice as a biodegradable alternative to conventional petrochemical-based polymers. Considerable progress has recently been made in developing high-yielding fermentation strategies primarily based on *E. coli* and *Alcaligenes eutrophus* [15, 20]. However, the negative aspect of this is the cost of PHA which is still high to reach a full commercialization and must be further reduced in order for the microbial route to be competitive [6, 22, 35].

Besides the cost of carbon substrates, when the oxygen transfer limitation is avoided during the later stages of the fed-batch fermentation, the cost is also extremely expensive [35], and it generally requires vessel pressurization, high mixing energy, high gas flow rates, and oxygen-enriched air feeds. All of these conditions increase the production cost substantially, particularly in large-scale industrial systems. Significant cost savings are possible when reduced oxygen-availability can be tolerated without any substantial drop in productivity. It has recently been shown that moderate oxygen limitation in pH-stat fed-batch fermentations of recombinant *E. coli* does not substantially hinder PHB productivity [40]. Under fully aerobic conditions, 149 g/l of PHB was obtained in a defined medium. The corresponding yields under oxygen-limited (1–3% dissolved oxygen concentration) and anaerobic conditions during the PHB-production phase were 157 g/l and 101 g/l, respectively. According to the results, it can clearly state that the oxygen-limited conditions do offer a much better outlook.

A cursory examination of the cellular metabolism indicates that oxygen-limited conditions may not reduce the PHB productivity for the following reasons which are stated below:

(1) Cell-growth reduction is recognized during the PHB accumulation phase in a typical fed-batch fermentation. This will lead to a significant decrease in the ATP demand (PHB synthesis does not require ATP), with a concomitant increase in the pseudo-steady-state concentration of the intracellular NADH. The cell must therefore reduce in the ATP generation by oxidative phosphorylation while still regenerating NAD^+ and/or restricting the production of NADH. This is facilitated by the partial activation of anaerobic pathways and changes in the pattern of oxidative

*Corresponding author
Phone: 82-42-869-3930; Fax: 82-42-869-3910;
E-mail: leesy@sorak.kaist.ac.kr
[†]These authors contributed equally to this work.

phosphorylation under conditions of low level of dissolved oxygen. For example, the aerobic and anaerobic pathways for pyruvate conversion to acetyl-CoA may be operating simultaneously [2]. The anaerobic pathway has an advantage because NADH is not formed. Activation of this pathway reduces the net amount of NADH formed per glucose molecule which is converted to acetyl-CoA (the precursor for PHB formation), thus reducing the need for reoxidation and possibly facilitating the microbial redox balance. This practical consequence reduces oxygen usage with unimpaired PHB productivity.

(2) In *A. eutrophus*, PHB production is putatively governed by the intracellular concentration of NADH [17, 27]. At high NADH levels, citrate synthase is inhibited, blocking entry of acetyl-CoA into the TCA cycle. Hence, acetyl-CoA accumulates in the expense of free CoA. This enhances the activity of the first PHB enzyme (3-ketothiolase), which is inhibited by CoA. Thus the increased intracellular NADH concentration under oxygen-limited conditions may improve PHB production. A recent study using *E. coli* showed that the activity of citrate synthase is significantly inhibited by NADH concentrations greater than 0.2 mM [18], while increasing the flow of acetyl-CoA which was into the PHA biosynthesis pathway. However, there were also strong interaction effects between NADH concentration and other variables such as NADPH/$NADP^+$ ratio.

This short examination was conducted to find out what the cellular response is to oxygen-limited conditions. It leads to numerous questions regarding the flux in each of the metabolic pathways during the PHB synthesis. Detailed examination of the metabolic fluxes, and ultimately the relationship of these fluxes to operating conditions and enzyme levels, will facilitate further improvements in the PHB production by fermentation. Therefore, in this study, we searched to quantitate the flux in key pathways during the PHB production. In fact, this was done by using the metabolic flux analysis (MFA), which is a sub-branch of the increasingly-popular field of metabolic engineering [1, 11, 12, 24, 25, 26, 28, 32, 33]. MFA has been used to examine a range of biological systems, including *E. coli* [36], hybridomas [3, 42], *Penicillium chrysogenum* [14], yeasts [34], and *Corynebacterium glutamicum* [30, 31]. However, the method has not been used to examine the formation of PHB in a recombinant *E. coli*. This information will indeed prove to be useful for a wide range of recombinant *E. coli* processes as well as for providing insights into the formation of PHB in oxygen-limited large-scale bioreactors.

Modeling and Theoretical Aspects

Biochemical Network

An overall view of the metabolic network is shown in Fig. 1.

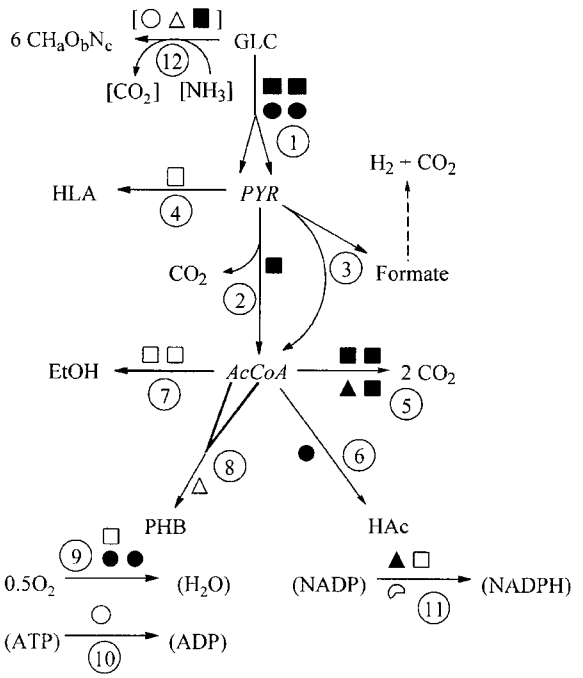

Fig. 1. Pictorial representation of the flux network, with flux labels shown in open circles. Cofactor requirements are indicated by ○=ATP, □=NADH, △=NADPH. Open shapes indicate consumption (of ATP, NADH, or NADPH), filled shapes indicate production. ⌒ indicates generation of 2/3 ATP, [] indicate variable cofactor requirements.

Glycolysis. Import of glucose and conversion to pyruvate via the phosphotransferase system is represented by flux F1, which includes the use of the pentose phosphate pathway (PPP) for NADPH generation (see "Anabolic Reactions").

$$Glc+2ADP+2NAD^+ \rightarrow 2PYR+2NADH+2ATP \quad (F1)$$

Pyruvate Catabolism. *E. coli* possesses two key enzymes for pyruvate conversion to acetyl-CoA (AcCoA) [2, 16]. Oxidative decarboxylation by pyruvate dehydrogenase (PDH) generates NADH and it has characteristics of being generally restricted to aerobic conditions. Under anaerobic conditions, pyruvate is converted to AcCoA by pyruvate-formate lyase (PFL), with the formation of formate. At a medium redox potential between true aerobic and anaerobic, both enzymes may be functional in metabolizing pyruvate [2].

$$PYR+NAD^+ \xrightarrow{PDH} AcCoA+CO_2+NADH \quad (F2)$$

$$PYR \xrightarrow{PFL} AcCoA+Formate \quad (F3)$$

Pyruvate-formate-lyase production is enhanced under anaerobic conditions [16]. Enzymatic conversion from its oxygen-stable inactive form to the oxygen-labile active form is stimulated by pyruvate and NADH.

Under anaerobic conditions, a formate-hydrogen lyase system (FHL) can potentially produce H_2 from formate [2],

$$\text{Formate} \xrightarrow{\text{FHL}} H_2+CO_2 \quad \text{(F3b)}$$

The FHL complex is synthesized at very low levels with neutral pH. As the pH level drops due to an acid product secretion, formate reaches a critical intracellular concentration level which results in an induction of the FHL production [2].

Production of lactate from pyruvate is also observed during an anaerobic fermentation. Under the pH-controlled batch fermentation, the amount of lactate formed should be minimal, although it definitely depends on certain environmental conditions [16]. A high PFL activity is the primary reason that the route to lactate is completely bypassed at a neutral or a basic pH range [16].

$$\text{PYR}+\text{NADH} \xrightarrow{\text{LDH}} \text{HLA}+\text{NAD}^+ \quad \text{(F4)}$$

Acetyl-CoA Catabolism. Acetyl-CoA (AcCoA) can flow into the tricarboxylic acid (TCA) cycle, where it is converted to NAD(P)H [42]:

$$\text{AcCoA}+3\text{NAD}^+ + \text{NADP}^+ \rightarrow 2CO_2+3\text{NADH}+\text{NADPH} \quad \text{(F5)}$$

AcCoA may also be converted to acetate (HAc) and excreted, via the acetate kinase (ack) and phosphotransacetylase (pta) enzymes:

$$\text{AcCoA}+\text{ADP} \leftrightarrow \text{HAc}+\text{ATP} \quad \text{(F6)}$$

The ack-pta pathway is enhanced by pyruvate, and repressed by NADH, ADP, and ATP [2].

Under conditions of low oxygen, NAD^+ regeneration may also occur via ethanol formation [16]:

$$\text{AcCoA}+2\text{NADH} \xrightarrow{\text{ADH}} \text{EtOH}+2\text{NAD}^+ \quad \text{(F7)}$$

ADH expression increases in response to a rise in an intracellular NADH/NAD^+ ratio, in an attempt to restore the internal redox balance by producing a highly-reduced ethanol [2].

Finally, poly(3-hydroxybutyrate) (PHB) is formed in a recombinant *E. coli* from AcCoA according to the equation F8 [20]:

$$2\text{AcCoA}+\text{NADPH} \rightarrow \text{PHB}+\text{NADP}^+ \quad \text{(F8)}$$

Although some NADH-dependent fatty-acid oxidation enzymes can supplement enzymes in this pathway, they have been ignored, because their activity is probably negligible compared to the recombinant enzymes. There is another possibility for this pathway to generate poly(3-hydroxyvalerate) from propionyl-CoA, which is produced in small amounts by *E. coli* cells. However, the amounts of PHV are negligible under the fermentation conditions employed in this study.

Oxidative Phosphorylation. Since *E. coli* has a flexible oxidative phosphorylation (OP) network, the ATP/NADH ratio is shown to be its variable. A figure of 2 ATP per NADH molecule is quite reasonable [10]:

$$\text{NADH}+\frac{1}{2}O_2+2\text{ADP} \rightarrow \text{NAD}^+ + 2\text{ATP} \quad \text{(F9)}$$

ATP usage for maintenance and futile cycling (if any) is represented by the equation F10:

$$\text{ATP} \rightarrow \text{ADP} \quad \text{(F10)}$$

Anabolic Reactions. Anabolic reactions generally require NADPH, which is primarily generated in three ways by *E. coli*, and they are: the TCA cycle, the pentose phosphate pathway, and ATP-linked NAD(P)H transhydrogenase. Stoichiometric analysis cannot readily distinguish between the latter two pathways, hence NADPH generation by these has been lumped into flux F11,

$$\text{NADH}+\text{NADP}^+ + \frac{2}{3}\text{ATP} \rightarrow \text{NAD}^+ + \text{NADPH} + \frac{2}{3}\text{ADP} \quad \text{(F11)}$$

This introduces a small error in ATP generation and hence flux F10.

Biomass formation in a minimal media requires an uptake of ammonia and substrate, net consumption of ATP and NADPH, and net production of NADH and CO_2:

$$(1+\alpha_C)\text{Glc}+\alpha_N NH_3+\gamma_N\text{NAD}^+ + \gamma_P\text{NADPH}+\gamma_A\text{ATP} \rightarrow 6CH_aO_bN_c+6\alpha_C CO_2+\gamma_N\text{NADH}+\gamma_A\text{ADP}+\gamma_P\text{NADP}^+ \quad \text{(F12)}$$

where *a*, *b*, and *c* are determined from an elemental analysis of the biomass. The ATP, NAD^+, and NADPH requirements can be expressed in terms of yield coefficients:

$$\gamma_A=6[12+a+16b+14c]Y_{xATP} \quad (1)$$

$$\gamma_N=6[12+a+16b+14c]Y_{xNAD} \quad (2)$$

$$\gamma_P=6[12+a+16b+14c]Y_{xNADPH} \quad (3)$$

For *E. coli* B/r cells growing in a minimal glucose medium at 37°C, with a 40 min doubling time, Y_{xATP} is 35.7×10^{-3} mol ATP/g (dry cells), Y_{xNAD+} is 20.5×10^{-3} mol NAD^+/g(dry cells), and Y_{xNADPH} is 14.6×10^{-3} mol NADPH/g (dry cells) [13]. For cells accumulating PHB, a dry cell weight in the yield coefficients is equivalent to the residual cell mass (RCM). RCM is defined as a dry cell weight (g/l) minus PHB concentration.

It is important to mention that carbon dioxide requirement for biomass synthesis is difficult to quantify. Ingraham *et al.* [13] provided tables of cofactor and carbon dioxide requirements for biomass assembly from twelve simple 'building blocks' such as acetyl-CoA and erythrose-4-phosphate. Assuming that synthesis of 1 mole of ribose-5-phosphate or acetyl-CoA produces 1 mole of CO_2,

synthesis of erythrose-4-phosphate produces 2 moles of CO_2, and synthesis of 1 mole of oxaloacetate requires 1 mole of CO_2, thus giving an estimation of 2.7 mmol of CO_2 produced per g RCM, and hence

$$\alpha_C=[12+a+16b+14c]\times 0.0027 \quad (4)$$

Unfortunately, the coefficients in the biomass equation (γ_A, γ_N, and γ_P) display a significant uncertainty, because the average macromolecular composition of the residual cell mass is likely to be altered during the fermentation process. The effect of the uncertainties will cause systematic errors in estimating some fluxes (in particular, F9, F10, F11) when biomass production is rapid. This topic is discussed subsequently and the coefficients are subjected to sensitivity tests.

Comments on Biochemical Network

The network does not explicitly include cellular maintenance requirements. Maintenance loads (both growth- and non-growth-associated) are represented by the flux through the ATP to ADP pathway (Flux F10). This equation is primarily introduced to open the ATP balance, which caused an uncertainty in the oxidative phosphorylation stoichiometry and the ATP requirements for biomass formation [3, 4].

A previous theoretical study has used linear optimization techniques mainly to predict the by-product secretion of *E. coli* under a variety of different levels of oxygen supply [39]. The criterion used was maximization of growth (generally limited by ATP production) whilst satisfying the redox constraints. When the available oxygen was decreased, acetate was the first byproduct to be secreted. At some oxygen supply level below this, both formate and acetate excretion were predicted. Finally, at highly oxygen-limited conditions, ethanol was also secreted. Lactate and succinate were not known to be excreted under any conditions. The predictions qualitatively matched the experimental data cited by the paper.

The network as described above has three degrees of freedom, viz. an NADH balance, an overall carbon balance, and a nitrogen balance. However, because of several practical limitations, the actual network used for flux analysis is a subset of the equations described above. First of all, the rate of oxygen consumption was not accurately measured due to calibration problems, and therefore was calculated from the NADH balance instead. Secondly, the flux (if any) through flux F3b formate-hydrogen-lyase cannot be accurately quantified unless the rate of hydrogen production is measured. If oxygen consumption had been measured, FHL quantification would theoretically be possible via an NAD(P)H balance but, in practice, this would be unwise since it is known to be very sensitive to errors in the rate measurements. Furthermore, as described earlier, the flux is likely to be negligible at a neutral pH. Therefore, it is not included in the network. Finally, ammonia uptake was not explicitly included in the network because of extreme uncertainty in the biomass nitrogen content, and the fact that nitrogen is not incorporated into any other metabolite in the model.

Flux Analysis

The reaction network and stoichiometry may be written in standard matrix notation for flux analysis [26]:

$$\mathbf{A}\mathbf{x}=\mathbf{r} \quad (5)$$

where $\mathbf{A}$ is the stoichiometric matrix embodying a mass balance on each metabolite, $\mathbf{x}$ is a column vector of fluxes, and $\mathbf{r}$ is a column vector of metabolite accumulation rates. For the network in this work, the pseudo-steady-state approximation for intracellular species has been applied and all other metabolites in the model except O_2 are measured. $\mathbf{A}$ is thus firstly partitioned into rows corresponding to measured (m), calculated (c), and pseudo-steady-state intracellular (p) metabolites. The pseudo-steady-state approximation leads to linear dependencies amongst the fluxes, hence row reduction is used on $\mathbf{A}_p$ to obtain an equation 6

$$\begin{pmatrix} \mathbf{A}_{md} & \mathbf{A}_{mi} \\ \mathbf{A}_{cd} & \mathbf{A}_{ci} \\ \mathbf{I} & \mathbf{A}_{pi} \\ \underline{\mathbf{0}} & \underline{\mathbf{0}} \end{pmatrix} \begin{pmatrix} \mathbf{x}_d \\ \mathbf{x}_i \end{pmatrix} = \begin{pmatrix} \mathbf{r}_m \\ \mathbf{r}_c \\ \underline{\mathbf{0}} \\ \underline{\mathbf{0}} \end{pmatrix} \quad (6)$$

where $\mathbf{A}$ has also been columnwise partitioned into dependent and independent fluxes. $\mathbf{A}_{pi}$ is the matrix relating the dependent and independent fluxes, viz.

$$\mathbf{I}\cdot\mathbf{X}_d+\mathbf{A}_{pi}\cdot\mathbf{x}_i=\underline{\mathbf{0}} \quad (7)$$

Estimates of the reaction fluxes may be obtained by least squares regression for the overdetermined system:

$$\mathbf{x}=\begin{pmatrix} \mathbf{x}_d \\ \mathbf{x}_i \end{pmatrix}=\begin{pmatrix} -\mathbf{A}_{pi}(\mathbf{T}^T\mathbf{E}_m^{-1}\mathbf{T})^{-1}\mathbf{T}^T\mathbf{E}_m^{-1}\mathbf{r}_m \\ (\mathbf{T}^T\mathbf{E}_m^{-1}\mathbf{T})^{-1}\mathbf{T}^T\mathbf{E}_m^{-1}\mathbf{r}_m \end{pmatrix} \quad (8)$$

where

$$\mathbf{T}=\mathbf{A}_{mi}-\mathbf{A}_{md}\mathbf{A}_{pi} \quad (9)$$

and $\mathbf{E}_m$ is the variance-covariance matrix of the measured accumulation rates.

Calculated rates (in particular, oxygen consumption) are obtained from

$$\mathbf{r}_C=\mathbf{A}_C\mathbf{x} \quad (10)$$

Estimates of the flux errors are given by the flux variance-covariance matrix:

$$\mathbf{E}_X=(\mathbf{C}_i-\mathbf{A}_{pi}\mathbf{C}_d)\mathbf{E}_{Xi}(\mathbf{C}_i-\mathbf{A}_{pi}\mathbf{C}_d)^T \quad (11)$$

where

$$\mathbf{F}_{Xi}=(\mathbf{T}^T\mathbf{F}_m^{-1}\mathbf{T})^{-1} \quad (12)$$

$$\mathbf{x}=\begin{pmatrix}\mathbf{x}_d\\ \mathbf{x}_i\end{pmatrix}=\underline{\mathbf{C}}_i\mathbf{x}_i+\underline{\mathbf{C}}_d\mathbf{x}_d \quad (13)$$

$$\underline{\mathbf{C}}_i=\begin{pmatrix}\underline{\mathbf{0}}\\ \mathbf{I}\end{pmatrix}, \text{ dimensions } \dim(\mathbf{x})\times\dim(\mathbf{x}_i) \quad (14)$$

$$\underline{\mathbf{C}}_d=\begin{pmatrix}\mathbf{I}\\ \underline{\mathbf{0}}\end{pmatrix}, \text{ dimensions } \dim(\mathbf{x})\times\dim(\mathbf{x}_d) \quad (15)$$

Gross errors, in either the stoichiometry or the measured rates, are indicated when h_δ does not follow the $\chi^2_{rank(F_{xi})}$ statistic [32, 33], where:

$$h_\delta=\underline{\delta}^T(\underline{\Delta}\mathbf{F}_m\underline{\Delta}^T)^{-1}\underline{\delta} \quad (16)$$

$$\underline{\Delta}=\mathbf{I}-\mathbf{T}(\mathbf{T}^T\mathbf{F}_m^{-1}\mathbf{T})^{-1}\mathbf{T}^T\mathbf{F}_m^{-1} \quad (17)$$

$$\underline{\delta}=\underline{\Delta}\mathbf{r}_m \quad (18)$$

The lumped metabolic pathways used in this model are shown pictorially in Fig. 1. A point to mention is that there is one degree-of-freedom: an overall carbon balance.

MATERIALS AND METHODS

Bacterial Strain and Plasmid

Recombinant *E. coli* strain XL1-Blue (*supE44 hsdR17 recA1 endA1 gyrA96 thi relA1 lac F' (proAB+ lacIq lacZΔM15Tn10(tet^r)*) harboring pSYL107 was used in this study [40]. The plasmid pSYL107 contains the *A. eutrophus* PHA biosynthesis genes, an *E. coli ftsZ* filamentation-suppression gene, the *parB* locus for plasmid stability, and an ampicillin resistance gene [19].

Medium and Culture Conditions

A single fed-batch high-cell-density fermentation was conducted with no deliberate oxygen restriction. Stock culture was stored in 20% (v/v) glycerol at -70°C before it was used to inoculate two 1-l shake flasks. Each shake flask contained 0.2 l MR-medium [40] supplemented with 20 g/l glucose, 0.1 g/l ampicillin, and 0.01 g/l thiamine. Then, after it was incubated for 30 h at 30°C and 250 rpm, the culture (total of 0.4 l) was used to inoculate a 6.6-l Bioflo 3000 bioreactor (New Brunswick Scientific Co., Edison, NJ, U.S.A.) that consisted of 1.2 l of initial medium with the same composition as the seed culture. Culture temperature was controlled at 30.0±0.5°C. Automatic feeding of 25% ammonia water took place when the pH level fell below 6.9. The amount added was measured by using an electronic mass balance. Foam was controlled manually by adding 30% (v/v) Antifoam 289 (Sigma Chemical Co., St. Louis, MO, U.S.A.) which was required. Possible dissolved oxygen was maintained above 20% by automatically varying agitation speed (maximum 1000 rpm). The inlet gas consisted of a mixture of both air and bottled oxygen. During the fermentation process, gas flowrate was held constant at 4 l/min and its oxygen concentration was increased as required, in discretion, and the bioreactor was not pressurized.

Batch cultivation was used until the initial glucose charge was depleted. As a result, nutrient feeding solution (700 g/l glucose, 15 g/l $MgSO_4 \cdot 7H_2O$, 0.25 g/l thiamine) was added by employing a pH-stat feeding strategy [21]. When the pH rose above 7.0, an appropriate amount of feeding solution was added automatically to restore the glucose concentration in the culture medium to 20 g/l. This feeding volume was calculated on-line by using a computer software (AFS3.42, New Brunswick Scientific Co.).

Analytical Procedures

Cell growth was monitored by measuring the optical density at 600 nm (OD_{600}) using a spectrophotometer (Beckman DU®650, CA, U.S.A.). The composition of outlet gas from the bioreactor was measured online by using a mass spectrometer (HAL Quadrupole mass spectrometer, Warrington, England). Representative samples of inlet gas were measured offline by the same mass spectrometer. Cell concentration, defined as dry cell weight (DCW), was determined as described previously [23]. PHB concentration was determined using a gas chromatograph (HP5890, Hewlett-Packard, Wilmington, DE, U.S.A.) with *n*-butyric acid as the internal standard [5]. Residual cell mass (RCM) is defined as DCW (g/l) minus PHB concentration (g/l). PHB content (%) is defined as the ratio of PHB concentration to the cell concentration. Elemental analysis of the sample was determined as follows: 25 ml of culture broth was centrifuged at 2100 ×g for 40 min, and the supernatant was discarded. The pellet was resuspended in distilled water and centrifuged again (2x). The final pellet was dried to maintain its constant weight in an oven at 60°C and was grounded into powder. An elemental analyzer (CE Instruments, Italy) was used to analyze carbon, hydrogen, oxygen, nitrogen, and sulfur compositions.

Concentrations of formic acid, lactic acid, and acetic acid in the culture medium were measured by HPLC (Hitachi L-3300 RI monitor, L-600 pump, D-2500 chromato-integrator, Tokyo, Japan) using an ion-exchange column (Aminex® HPX-87H, 300 mm×7.8 mm, Hercules, CA, U.S.A.) with 0.01 N H_2SO_4 for the mobile phase. Enzymatic test kits were used to measure concentrations of glucose (Yeongdong Pharmaceutical Corp, Korea), ethanol (Boehringer Mannheim, Mannheim, Germany), ammonia (Boehringer Mannheim, Mannheim, Germany), and carbon dioxide (Sigma Diagnostics, U.S.A.) in the culture medium.

RESULTS AND DISCUSSION

Preliminary Linear Optimization

Analogous to the theoretical study [39] mentioned in Modelling and Theoretical Aspects, simple linear optimization was conducted on the network mainly to investigate the flux distribution necessary to acquire a maximum possible PHB production. Under conditions of ample oxygen and no biomass formation, 100 mol of glucose was converted into 100 mol of PHB. ATP available for maintenance was 733 mol. In addition, 150 mol of O_2 was utilized and 200 mol of CO_2 was produced (RQ=1.33). When the oxygen supply was limited in a range of 50-150 mol (RQ=4.0 to 1.33, respectively), the PFL (and FHL) pathway could theoretically be compensated by substituting H_2 generation for NADH generation, with no reduction in an efficiency of carbon conversion to PHB. Below 50 mol O_2 (RQ>4.0), ethanol secretion occurred, with concomitant reduction in the carbon conversion efficiency. At zero O_2 flux, 200 mol of CO_2 and 67 mol each of ethanol and PHB were produced, with only 156 mol of ATP being available. Neither TCA cycle operation nor acetate secretion was predicted unless a lower limit was set on the ATP production. A word to mention is that lactate secretion was not predicted. This preliminary result supports the assertion in the introduction that high PHB productivity can be maintained under oxygen-limited conditions, with associated savings in aeration costs [35], and justifies the subsequent experimental study.

General Comments on Experimental Results

Figure 2 shows the time profiles of PHB content and PHB, RCM, and DCW concentrations. The final dry cell weight was 227 g · l^{-1} with a final PHB content of 78% (=177 g · l^{-1} PHB). Despite its slow growth rate (initially 0.3 h^{-1}), the overall reactor productivity was 3.39 g (PHB) · l (broth)$^{-1}h^{-1}$ on the minimal medium. An overall yield of PHB obtained on glucose was 75% mol (PHB)/mol (glucose), or 36% on a mass basis. Figures 3 and 4 show that from 28 h onwards, where residual cell mass reached its plateau, PHB yield rose as much as 90% mol (PHB)/mol (glucose). This is very similar to the 100% (mol/mol) or 48% (w/w) theoretical maximum ratio predicted by Yamane [41], in which it does not include biomass formation or byproduct secretion. The yield of RCM on glucose remained constant at 45% g (RCM)/g (glc), as estimated over the first 15 h. This shows a close comparison with a typical 40-50% (w/w) values obtained for non-recombinant *E. coli* [38]. The estimated respiratory quotient (RQ) was 0.90±0.05 for the first 18 h. RQ rose rapidly to 1.05 at 21 h, then slowly increased to 1.15 by 30 h and remained at 1.15±0.03 thereafter.

Figure 3 shows that initially the PHB synthesis rate was negligible and cell growth rate was comparatively high. A specific growth rate was 0.3 h^{-1} (doubling time 2.3 h). However, it dropped sharply to zero within 15 to 23 h as PHB production rate climbed. Eventually, the cell mass production ceased at approximately 29 h and became slightly negative, and this was probably due to lysis and/or breakdown of cell components for re-use.

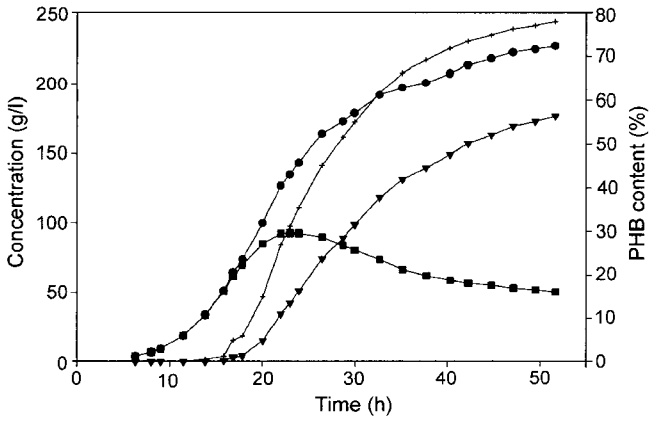

Fig. 2. Time profiles of Poly(3-hydroxybutyrate) concentration (-▲-), dry cell weight concentration (-●-), residual cell mass concentration (-■-), and cellular Poly(3-hydroxybutyrate) content (-×-).

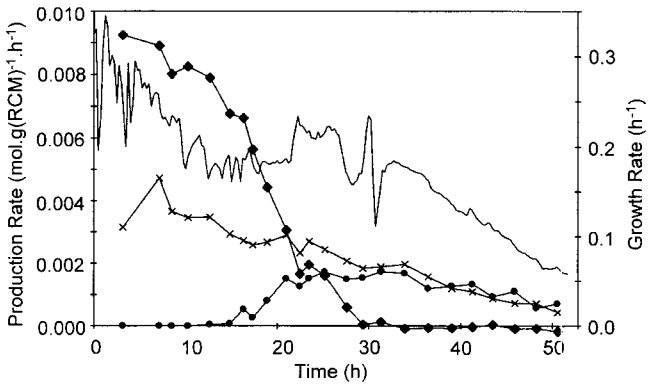

Fig. 3. Specific production/consumption rates of Poly(3-hydroxybutyrate) (-●-), glucose (-×-), CO_2 (——), and residual cell mass (-◆-).

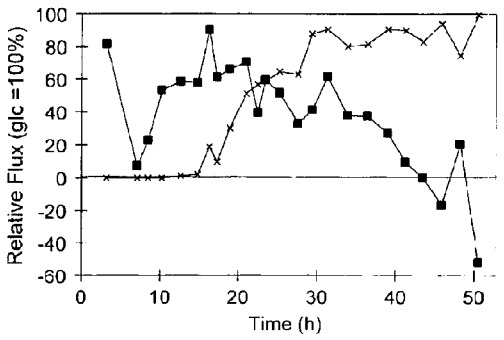

Fig. 4. Time profile of Poly(3-hydroxybutyrate) (F8=-×-) and ATP-linked NAD(P)H transhydrogenase (F11=-■-) fluxes, relative to the glucose uptake flux.

Aspects of Oxygen Usage

Figure 5 shows the dissolved oxygen concentration throughout the fermentation. Large spikes are a result of the pH-stat nutrient feeding used, since each time glucose exhausted there was a brief period of growth on acetate before the next feeding pulse. At this time, cellular oxygen usage is reduced, causing a rise in a dissolved oxygen concentration. From 26 h to 29 h, oxygen demand was high enough that it was not necessary for spikes to be observed. Several other events occurred during this period as shown by Figs. 3, 6, 7, and 8: the residual cell mass production declined to zero, and rapid production of acetate and lactate occurred. Oxygen restriction seems to be the likely cause of this reaction. At approximately 29 h, cell growth ceased entirely and the specific PHB production rate reached a maximum level. During this hour, oxygen consumption decreased as proven by the increased dissolved oxygen level, the CO_2 production rate was also temporarily elevated for a short period of time. Lactate was also rapidly remetabolized by the cell; however, for reasons that are not known, pH did not rise and nutrient feeding was not triggered. After 30 h, nutrient feeding and oxygen consumption returned to their prior levels. Fluxes to or from the acids were then slowed down until 40 h when acetate production recommenced. Aerobic acetate excretion seems to occur in *E. coli* at high growth rates. Various studies suggest that this is caused by a mismatch between the glycolytic and TCA fluxes, which in turn leads to excessive intracellular acetyl-CoA concentration [9]. The comparatively low levels of excretion observed in this fermentation suggest that PHA biosynthesis may reduce acetate excretion by withdrawing excess acetyl-CoA.

Experiments with *E. coli* B/r (wild-type) have shown that during a balanced growth period, a specific oxygen uptake rate is approximately the same (20 mmol (O_2) per g (DCW) per h) for many different substrates and growth rates [13]. An estimated specific oxygen consumption rate for this fermentation was between 8-9 mmol/g(RCM)/h over the first 15 h. Thereafter, it declined steadily up to nearly 1.5 mmol/g(RCM)/h by 50 h. Since growth rate decreases steadily when PHB accumulates intracellularly, this explains the reason for the decrease in the cellular oxygen demand. An assumption was made that many cells begin to die once the total residual cell mass reached a plateau, which resulted in a further decrease in oxygen requirements. It is important to note that PHB synthesis is rapid and efficient even under this reduced oxygen demand.

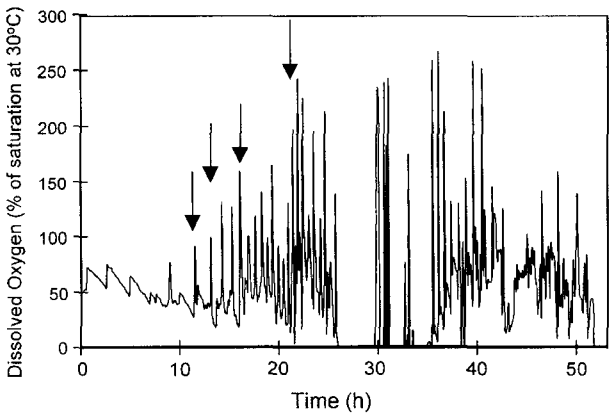

Fig. 5. Dissolved oxygen content throughout the fermentation. Arrows refer to an increase in the oxygen content of the inlet gas, from 21% to 28.8%, 40.4%, 67.5%, and 98.5%, respectively. Gas flow rate was constant at 4.0 l (STP)/min and the fermenter was not pressurized.

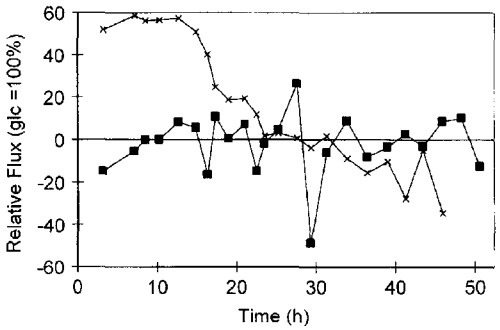

Fig. 7. Time profile of lactate (F4= ■) and biomass (F12= ×) fluxes relative to the glucose uptake flux.

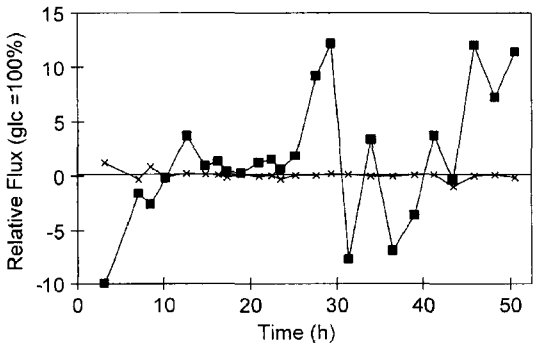

Fig. 6. Time profile of acetate (F6=—■—) and ethanol (F7=—×—) fluxes relative to the glucose uptake flux.

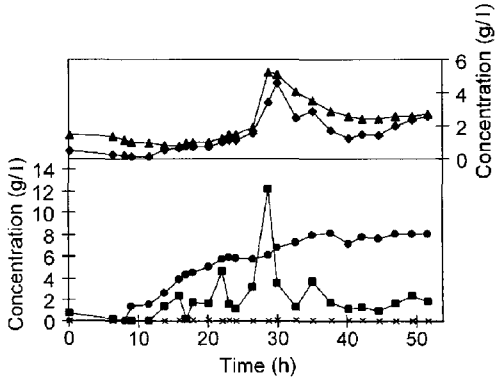

Fig. 8. Time profiles of acetate (—◆—), lactate (—■—), formate (—●—), ethanol (—×—), and ammonium (—▲—) concentrations.

Flux Analysis

Many of the fluxes in this model (eg. acetate flux) do not give much more information than for the excretion profiles themselves. However, two main benefits could be acquired from applying this simple metabolic flux analysis to the data: The firs benefit is that it allows for both carbon balance and data reconciliation. Secondly, it elucidates several key internal fluxes such as the TCA cycle flux and ATP generation. Figures 4, 6, 7, 9, and 10 show the calculated fluxes. Typical values for the flux standard deviations are given in Table 1. Singular value decomposition for each sample indicates that the system as defined is well conditioned. In general, it appears that random errors are not likely to qualitatively alter the results. A possibility of systematic errors are of a major concern and it should be discussed.

The byproduct excretion fluxes seem to be very interesting. A level of ethanol secretion was extremely low (100 mg · l^{-1} maximum) as expected, because its main usefulness to the cell is identified for maintaining redox balance when oxygen is unavailable. This result suggests that the oxygen supply during this fermentation was sufficient for maintaining a low NADH/NAD^+ ratio and thus avoiding ethanol production. Formate production was at its low point, and at a relatively constant fraction of the glucose flux (5-10%), apart from a period of rapid production near 8 h. This flux was unexpected because formate production is usually restricted to anaerobic conditions. Another point of interest is that, unlike lactate and acetate, formate was not reutilized by the cell after being excreted, apart from one datum point at 39 h. Lactate and acetate production appear to be well-correlated, except after 45 h when lactate production ceased while acetate excretion did not. Lactate was excreted to high concentrations, averaging 3 g/l and reached its peak at 12 g/l. This was also unexpected because lactate production is usually observed only at low pH levels and under anaerobiosis. In general, lactate is observed to appear last during batch culture, when acid secretion has significantly lowered the pH and (presumably) the production of other organic acids is inhibited by end products [2]. This is also supported by the results of the Preliminary Linear Optimization section above. However, the LDH activity is enhanced by pyruvate. Hence, FHL and LDH may have been activated by a high pyruvate concentration, caused for example by a restricted flux through pyruvate dehydrogenase.

The lactate and formate excretion during 0 h to 20 h may also reflect the oxygen limitation, despite of the measured dissolved oxygen concentration level being above 20% of the saturation level. Mass-transfer resistance and imperfect mixing can lead to large, rapid fluctuations in the oxygen available to the cell, and dissolved-oxygen-probes do not detect such fluctuations.

The TCA cycle flux is of great interest because it competes with the PHB pathway for acetyl-CoA. Figure 9 shows that the TCA cycle flux (relative to glucose uptake) is initially high, coinciding with a period of rapid biomass synthesis. Thereafter, it decreases somewhat linearly until the point of maximum PHB production was reached, and then it begins to increase slowly once more. The reason for this increase is unclear. Figure 10 also shows that the ATP dissipation relative to the glucose flux increases steadily

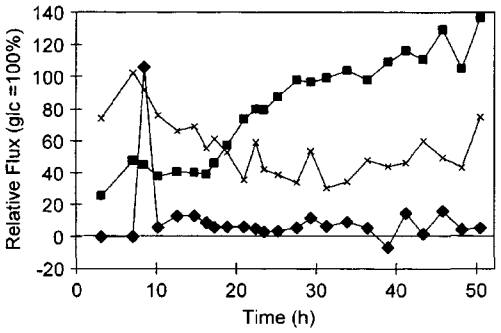

Fig. 9. Time profile of glycolysis (F1=-■-), TCA (F5=-×-), and formate (F3=-◆-) fluxes, relative to the glucose uptake flux.

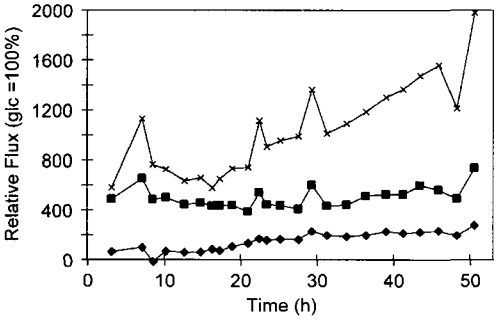

Fig. 10. Time profile of pyruvate dehydrogenase (F2=-◆-), oxidative phosphorylation (F9=-■-), and ATP dissipation (F10=-×-) fluxes, relative to the glucose uptake flux.

Table 1. Typical estimated flux standard deviations as a percentage of the flux during various stages of the fermentation.

Flux	Early (0-15 h)	Mid (15-35 h)	Late (35-52 h)
1	4%	5%	30%
2	4%	5%	30%
3	7%	25%	75%
4	10%	20%	40%
5	4%	20%	60%
6	20%	25%	40%
7	20%	35%	10%
8	4%	10%	60%
9	4%	8%	20%
10	6%	9%	12%
11	7%	35%	80%
12	1%	7%	-

throughout the fermentation period. This may reflect either a greater relative metabolic burden for maintenance due to the declining glucose flux, or conversely a greater level of futile cycling due to an excessive TCA cycle flux and ATP generation.

Potential Errors and Limitations

The test statistic usually lies within the 90% confidence limits, indicating that during most of the fermentation, the network adequately describes the observable rates and that measurement error estimates seem to be quite reasonable. As formulated, the flux network has one degree of redundancy, i.e. an overall carbon balance. Closure is excellent (typically 95% on a carbon-mol basis) in the middle period of the fermentation, between 14 h and 39 h. In the earlier stages, there is consistent under-detection of products, typically 10%, whereas excess carbon is produced in the final stages (from 20–60%). This may reflect excretion and subsequent reutilization of an undetected metabolite, such as succinate. Future experiments would elucidate this; however, an overall balance for the entire fermentation indicates some 5% of an excess carbon production. This must reflect a systematic error in one of the measurements, probably the CO_2 production rate since this forms a large portion of the carbon balance and is less accurately measured than glucose. Closure is poor for the two samples over 24 h to 29 h, where only about 10% extra carbon is detected. This coincides with the severe oxygen limitation period and, unfortunately, the significance of this (if any) is not apparent. In general, the flux most likely to be affected by the poor closure is the TCA flux F5, which is estimated from a carbon dioxide production. The systematic error must be slight in this study.

The data provided in this study are subjected to several other limitations that could be avoided in future works. The most major shortcoming is the absence of measured oxygen consumption, due to difficulties with calibration. Measuring oxygen would not only allow for NAD(P)H balance, but it would significantly improve the estimate of several key fluxes such as the TCA cycle and NADPH transhydrogenase fluxes as well. Another deficiency that emerged was poor closure of the nitrogen balance after 30 h; the uptake of ammonia continued steadily, without an appearance of biomass nitrogen. Most likely, this reflects a generation of an undetected nitrogen-containing metabolite, which could be detected by testing for kjehdahl nitrogen in the medium.

Sensitivity tests were conducted where the NADPH requirement for biomass production was varied by a factor of two factors in each direction from the assumed 14.6 mmol/g RCM. During the early stage, the corresponding variation in the flux F11 (NAD(P)H transhydrogenase) was often ±60% of the glucose flux. The middle stage was less sensitive. In general, biomass parameters are a cause for concern, because they are so poorly defined and are highly variable as changes shown in the RCM composition occur. The fluxes most severely affected by changes to the NADPH coefficient are flux F11 and flux F9 (calculated oxygen usage). For both NADPH and NADH, halving or doubling the coefficient changes flux F9 by about 100% of the glucose flux in each direction, or ±25% of the calculated oxygen usage. The ATP coefficient has a large effect on flux F10 (ATP dissipation), which varies by about 200% of the glucose flux. The CO_2 coefficient has negligible influence on any flux. In light of these inaccuracies, absolute values of fluxes F10 and F11 should be regarded with caution. Nevertheless, the general trends and relative comparisons between fluxes seem to be unaffected by these potential systematic errors.

Areas for Possible Optimization

The flux data suggest several different ways in which PHB production could be vastly improved. The production of formate is undesirable except perhaps under anaerobic conditions. Although this does not directly reduce the efficiency of PHB production, it may inhibit cell function, especially during the growth phase. It may also indicate a restriction of flux through pyruvate dehydrogenase. Lactate excretion should not be necessary when looking at it theoretically, and is possibly caused by a restricted flux to an acetyl-CoA (and hence PHB). If there is a possibility that the causes of excessive excretion could be removed, then it is more than likely that the PHB productivity can be improved.

As discussed previously, a sizeable fraction (15–25%) of the flux to acetyl-CoA enters the TCA cycle and is thereby wasted by converting to CO_2. This is reflected in the rate of oxidative phosphorylation as shown in Fig. 10, which remains at a high level despite cessation of growth and reduction in ATP requirements for biomass synthesis. If the TCA flux could be decreased during the latter stages of the fermentation, this may lead to an increase in the PHB production efficiency.

A significant disadvantage of existing high-cell-density fermentation protocols is that pure oxygen feed is required at high cell densities. Using air and allowing the culture to become oxygen-limited could provide a substantial economic benefit. During 26–30 h, where the dissolved oxygen concentration dropped to zero, neither PHB production rate (Fig. 3) nor carbon conversion efficiency (Fig. 4) appear to be impaired. Unfortunately, the flux data suggest that oxygen depletion may have caused both rapid lactate and acetate excretion. Although the direct effect on carbon efficiency was negligible, high levels of lactate and acetate can inhibit cellular function and thus potentially reduce the PHB production rate and efficiency. Further experiments are required to investigate system performance under more severely oxygen-limited conditions and allow better prediction of performance in scaled-up bioreactors.

CONCLUSIONS

Metabolic fluxes in key pathways were quantitatively analyzed during the PHB production by a high-cell-density fed-batch culture of the recombinant *E. coli*. High PHB accumulation (177 g/l PHB), cell PHB content (78%), and reactor productivity (3.39 g (PHB)/l (broth)/h) were obtained with a minimal glucose medium. The byproduct excretion time profiles differ quite markedly from those of typical wild-type strains described in the literature, both before and during the PHB production. In particular, a significant excretion of lactate and formate was unexpected. PHB production did not appear to be suppressed during periods of severe oxygen limitation; however, some increase in byproduct excretion was observed. Ethanol production was extremely low despite its oxygen limitation, probably due to the action of PHB as a NAD(P)H sink. In general, oxygen consumption seems to be considerably repressed relative to literature values for wild-type strains. Future work is suggested in order to examine the effect of further restricting oxygen supply during the PHB production phase. Such studies will assist in avoiding byproduct secretion, reducing oxygen requirement while maintaining its PHB productivity, and improving fermentation control.

Acknowledgments

A. P. J. Middelberg thanks the Australian Academy of Science and the Korea Science and Engineering Foundation for travel support under the bilateral exchange program, and the University of Adelaide for sabbatical support. This work was partly supported by the International Cooperative Program of the Ministry of Science and Technology, Korea; the Australian Research Council; and the Australian Dairy Research and Development Corporation.

Nomenclature

$\mathbf{A}$	Matrix of stoichiometric coefficients
$\mathbf{C}$	Flux concatenation matrix
$\mathbf{F}$	Variance-covariance matrix
$\mathbf{h}_\delta$	Residuals test statistic
$\mathbf{r}$	Vector containing rates of accumulation of metabolic species
$\mathbf{T}$	Reduced stoichiometric matrix
$\mathbf{x}$	Vector containing reaction fluxes
$\mathbf{Y}$	Cofactor requirements for biomass synthesis (mol per gram biomass)

Greek Symbols

α_C	Carbon dioxide stoichiometric coefficient in biomass equation
α_N	Ammonia stoichiometric coefficient in biomass equation
$\underline{\delta}$	Vector of residuals between predicted and measured rates
$\underline{\Delta}$	Redundancy matrix
γ_A	ATP stoichiometric coefficient in biomass equation
γ_N	NADH stoichiometric coefficient in biomass equation
γ_P	NADPH stoichiometric coefficient in biomass equation

Subscripts

c	calculated
d	dependent
i	independent
m	measured
p	pseudo-steady-state constraints
x	reaction fluxes

REFERENCES

1. Bailey, J. E. 1991. Toward a science of metabolic engineering. *Science* **25:** 1668-1675.
2. Böck, A. and G. Sawers. 1996. Fermentation, pp. 262-282. *In* F.C. Neidhardt *et al.* (eds.), *Escherichia coli and Salmonella: Cellular and Molecular Biology.* 2nd ed. ASM Press, Washington D.C., U.S.A.
3. Bonarius, H. P. J., V. Hatzimanikatis, K. P. H. Meesters, C. D. de Gooijer, G. Schmid, and J. Tramper. 1996. Metabolic flux analysis of hybridoma cells in different culture media using mass balances. *Biotechnol. Bioeng.* **50:** 299-318.
4. Bonarius, H. P. J., G. Schmid, and J. Tramper. 1997. Flux analysis of underdetermined metabolic networks: The quest for the missing constraints. *Trends Biotech.* **15:** 308-314.
5. Braunegg, G., B. Sonnleitner, and R. M. Lafferty. 1978. A rapid gas chromatographic method for the determination of poly-3-hydroxybutyric acid in microbial biomass. *Eur. J. Appl. Microbiol. Biotechnol.* **6:** 29-37.
6. Choi, J. and S. Y. Lee. 1997. Process analysis and economic evaluation for poly(3-hydroxybutyrate) production by fermentation. *Bioprocess Eng.* **17:** 335-342.
7. Cronan, J. E. and D. LaPorte. 1996. Tricarboxylic acid cycle and glyoxylate bypass, p. 206. *In* F. C. Neidhardt *et al.* (eds.), *Escherichia coli and Salmonella Typhimurium*, 2nd Ed. ASM Press, Washington D.C., U.S.A.
8. Gennis, R. B. and V. Stewart. 1996. Respiration, pp. 217-261. *In* F. C. Neidhardt (ed.), *Escherichia coli and Salmonella: Cellular and Molecular Biology.* 2nd ed. ASM Press, Washington D.C., U.S.A.
9. Goel, A., M. M. Domach, W. Hanley, J. W. Lee, and M. M. Ataai. 1995. Coordination of glycolysis and TCA cycle reaction networks. *Ann. NY Acad. Sci.* **782:** 2.
10. Harold, F. M. and P. C. Maolney. 1996. Energy transduction by ion currents, pp. 283-306. *In* F. C. Neidhardt *et al.* (eds.), *Escherichia coli and Salmonella: Cellular and Molecular Biology.* 2nd ed. ASM Press, Washington D.C., U.S.A.

11. Hatzimanikatis, V. and J. E. Bailey. 1997. Effects of spatiotemporal variations on metabolic control: Approximate analysis using (log) linear kinetic models. *Biotechnol. Bioeng.* **54:** 91-104.
12. Hu, W. S, W. Zhou, and L. F. Europa. 1998. Controlling mammalian cell metabolism in bioreactors. *J. Microbiol. Biotechnol.* **8:** 8-13.
13. Ingraham, J. L., O. Maaloe, and F. C. Neidhardt. 1983. *Growth of the Bacterial Cell.* Sinauer Associates, Sunderland, U.S.A.
14. Jørgensen, H., J. Nielsen, and H. Villadsen. 1995. Metabolic flux distributions in *Penicillium chrysogenum* during fed-batch cultivations. *Biotechnol. Bioeng.* **46:** 117-131.
15. Jung, Y. M. and Y. H. Lee. 1997. Investigation of regulatory mechanism of flux of acetyl-CoA in *Alcaligenes eutrophus* using PHB-negative mutant and transformants harboring cloned *phbCAB* genes. *J. Microbiol. Biotechnol.* **7:** 215-222.
16. Kessler, D. and J. Knappe. 1996. Anaerobic dissimilation of pyruvate, pp. 199-205. *In* F. C. Neidhardt *et al.* (eds.), *Escherichia coli and Salmonella: Cellular and Molecular Biology.* 2nd ed. ASM Press, Washington D.C., U.S.A.
17. Leaf, T. A. and F. Srienc. 1998. Metabolic modeling of polyhydroxybutyrate biosynthesis. *Biotechnol. Bioeng.* **57:** 557-570.
18. Lee, I. Y., M. Y. Kim, Y. H. Park, and S. Y. Lee. 1996. Regulatory effects of cellular nicotinamide nucleotides and enzyme activities on poly(3-hydroxybutyrate) synthesis in recombinant *Escherichia coli. Biotechnol. Bioeng.* **52:** 707-712.
19. Lee, S. Y. 1994. Suppression of filamentation in recombinant *E. coli* by amplified FtsZ activity. *Biotechnol. Lett.* **16:** 1247-1252.
20. Lee, S. Y. 1996. Bacterial polyhydroxyalkanoates. *Biotechnol. Bioeng.* **49:** 1-14.
21. Lee, S. Y. 1996. High cell-density culture of *Escherichia coli. Trends Biotechnol.* **14:** 98-105.
22. Lee, S. Y. 1996. Plastic bacteria? Progress and prospects for polyhydroxyalkanoate production in bacteria. *Trends Biotechnol.* **14:** 431-438.
23. Lee, S. Y., K. S. Yim, H. N. Chang, and Y. K. Chang. 1994. Construction of plasmids, estimation of plasmid stability, and use of stable plasmids for the production of poly(3-hydroxybutyric acid) in *Escherichia coli. J. Biotechnol.* **32:** 203-211.
24. Liao, J. C. and J. Delgado. 1993. Advances in metabolic control analysis. *Biotech. Progress* **9:** 221-233.
25. Liao, J. C., S.-Y. Hou, and Y.-P. Chao. 1996. Pathway analysis, engineering, and physiological considerations for redirecting central metabolism. *Biotechnol. Bioeng.* **52:** 129-140.
26. Nielsen, J. and J. Villadsen. 1993. *Bioreaction Engineering Principles.* Plenum Press, New York, U.S.A.
27. Oeding, V. and H. G. Schlegel. 1973. β-ketothiolase from *Hydrogenomonas eutropha* H16 and its significance in the regulation of poly-β-hydroxybutyrate metabolism. *Biochem. J.* **134:** 239-248.
28. Stephanopoulos, G. and J. J. Vallino. 1991. Network ridigity and metabolic engineering in metabolic overproduction. *Science* **252:** 1675-1681.
29. Stouthamer, A. H. 1973. A theoretical study on the amount of ATP required for synthesis of microbial cell material. *Ant. Leeuwenh.* **39:** 545-565.
30. Takiguchi, N., H. Shimizu, and S. Shioya. 1997. An online physiological state recognition system for the lysine fermentation process based on a metabolic reaction model. *Biotechnol. Bioeng.* **55:** 170-181.
31. Vallino, J. J. and G. Stephanopoulos. 1993. Metabolic flux distributions in *Corynebacterium glutamicum* during growth and lysine overproduction. *Biotechnol. Bioeng.* **41:** 633-646.
32. van der Heijden, R. T. J. M., B. Romein, J. J. Heijnen, C. Hellinga, and K. Ch. A. M. Luyben. 1994. Linear constraint relations in biochemical reaction systems: I. Classification of the calculability and balanceability of conversion rates. *Biotechnol. Bioeng.* **43:** 3-10.
33. van der Heijden, R. T. J. M., B. Romein, J. J. Heijnen, C. Hellinga, and K. Ch. A. M. Luyben. 1994. Linear constraint relations in biochemical reaction systems: II. Diagnosis and estimation of gross errors. *Biotechnol. Bioeng.* **43:** 11-20.
34. van Gulik, W. M. and J. J. Heijnen. 1995. A metabolic network stoichiometry analysis of microbial growth and product formation. *Biotechnol. Bioeng.* **48:** 681-698.
35. van Wegen, R. J., Y. Ling, and A. P. J. Middelberg. 1998. Industrial production of polyhydroxyalkanoates using *Escherichia coli*: An economic analysis. *Trans. IChemE* Part A. **76:** 417-426.
36. Varma, A., B. W. Boesch, and B. O. Palsson. 1993. Biochemical production capabilities of *Escherichia coli. Biotechnol. Bioeng.* **42:** 59-73.
37. Varma, A. and B. O. Palsson. 1993. Metabolic capabilities of *Escherichia coli*: I. Synthesis of biosynthetic precursors and cofactors. *J. Theor. Biol.* **165:** 477-502.
38. Varma, A. and B. O. Palsson. 1993. Metabolic capabilities of *Escherichia coli*: II. Optimal growth patterns. *J. Theor. Biol.* **165:** 503-522.
39. Varma, A., B. W. Boesch, and B. O. Palsson. 1993. Stoichiometric interpretation of *Escherichia coli* glucose catabolism under various oxygenation rates. *Appl. Environ. Microbiol.* **59:** 2465-2473.
40. Wang, F. and S. Y. Lee. 1997. Production of poly(3-hydroxybutyrate) by fed-batch culture of filamentation-suppressed recombinant *Escherichia coli. Appl. Environ. Microbiol.* **63:** 4765-4769
41. Yamane, T. 1993. Yield of Poly-D(-)-3-hydroxybutyrate from various carbon sources: a theoretical study. *Biotechnol. Bioeng.* **41:** 165-170.
42. Zupke, C. and G. Stephanopoulos. 1995. Intracellular flux analysis in hybridomas using mass balance and *in vitro* ^{13}C NMR. *Biotechnol. Bioeng.* **45:** 292-303.